# Carbene triel bonds between $TrR_3$ (Tr=B, Al) and N-heterocyclic carbenes

Zongqing Chi,[1] Wenbo Dong,[1] Qingzhong Li,[1,*] Xin Yang,[1] Steve Scheiner,[2,*] and Shufeng Liu[3]

[1]The Laboratory of Theoretical and Computational Chemistry, School of Chemistry and Chemical Engineering, Yantai University, Yantai 264005, People's Republic of China

[2]Department of Chemistry and Biochemistry, Utah State University, Logan, UT 84322-0300, USA

[3]Shandong Key Laboratory of Biochemical Analysis; College of Chemistry and Molecular Engineering, Qingdao University of Science and Technology, Qingdao 266042, PR China

**Corresponding authors**: Qingzhong Li and Steve Scheiner

E-mail: liqingzhong1990@sina.com and steve.scheiner@usu.edu

**Abstract**

The carbene triel bond is predicted and characterized by theoretical calculations. The C lone pair of N-heterocyclic carbenes (NHCs) is allowed to interact with the central triel atom of $TrR_3$ (Tr = B and Al; R = H, F, Cl, and Br). The ensuing bond is very strong, with an interaction energy of nearly 90 kcal/mol. Replacement of the C lone pair by that of either N or Si weakens the binding. The bond is strengthened by electron-withdrawing substituents on the triel atom, and the reverse occurs with substitution on the NHC. However, these effects do not strictly follow the typical pattern of F > Cl > Br. The $TrR_3$ molecule suffers a good deal of geometric deformation, requiring on the order of 30 kcal/mol, in forming the complex. The R(C···Tr) bond is quite short, e.g. 1.6 Å for Tr=B, and shows other indications of at least a partially covalent bond, such as a high electron density at the bond critical point and a good deal of intermolecular charge transfer.

**Keywords**: Silylene; Imidazole; Substituent effects; Carbene triel bond

## 1. INTRODUCTION

The successful isolation and characterization of N-Heterocyclic carbenes (NHCs), one of the success stories of recent research, opened up a new class of organic compounds in organometallic[1-4] and organocatalysts.[5-7] Herrmann and Köcher presented an earlier review of the synthesis, structure, bonding theory, metal coordination chemistry, and catalysis of NHCs.[1] It is understood that NHCs bind not only to transition metal atoms, in both low and high oxidation states, as well as to main group elements such as sulfur, iodine, and beryllium.[2] In particularly, NHC–gold complexes have extensive applications in the context of potential drugs, luminescent devices, and homogeneous and heterogeneous catalysts.[[3]] NHC–metal complexes can stabilize highly reactive intermediates and thus promote constructive chemical steps at the metal center.[4] Two reviews in 2007 highlighted the numerous applications of imidazolylidene, imidazolinylidene, triazolylidene, and thiazolylidene inorganocatalysis.[5,6] These works have been supplemented by a recent review that summarizes the newest and most exciting applications of NHCs.[7]

In other applications, carbenes have been used as electron donors in various types of intermolecular interactions.[8-18] Like other sorts of electron donors,[19] intermolecular interactions involving carbenes are also taken as a preliminary stage of a reaction,[16,17] particularly for NHCs. NHCs also act as a trap for carbon dioxide by forming a non-covalent interaction or covalent bonding adduct.[18] A new sensor for the fluorescent and colorimetric detection of carbon dioxide has been established by means of the fluoride-induced formation of an N-heterocyclic carbene intermediate that reacts with carbon dioxide to form an imidazolium carboxylate.[20] NHCs engage in a strong carbene tetrel bond with $TH_3F$ in the order of T = C < Ge < Sn < Si, different from the pattern observed with $CH_2$.[15] These results suggest that NHCs can engage in particularly strong intermolecular interactions.

From another direction, it has been demonstrated that $BR_3$ (R = H or halogen) can bind strongly to Lewis bases such as HCN, $CH_3CN$, and $NH_3$.[21-29] The strength of this bonding has been attributed in a large part to the electron-deficiency of a trivalent triel atom, making it a strong Lewis acid. Another property evoking interest in such complexes is their unusually large differences in gas and solid structures. Specifically, crystallization changes the B-N bond length and NBX angle a great deal. Another perhaps surprising finding is that $BH_3$ engages in a stronger intermolecular binding than does $BF_3$, despite the greater electron-withdrawing power of F which ought to make $BF_3$ a more potent Lewis acid. An early explanation of this apparent contradiction resorted to the phenomenon of backbonding, wherein the halogen atom donates π electron density into the empty 2p orbital of the $sp^2$-hybridized boron atom.[30] Grabowski recently presented a more nuanced explanation involving polarization.[31] $BR_3$ exhibits a region of positive molecular electrostatic potentials (MEPs) above the molecular plane, a so-called π-hole[32] which can attract the negative

segment of a partner molecule, a Lewis base. In a more general sense, the non-covalent bonding involving any triel atom, B, Al, etc is generally referred to as triel bonding.[32] It is generally found that the planar trigonal structure of $TrR_3$ is modified toward a tetrahedral geometry within a triel-bonded complex, and toward a trigonal bipyramid if two bases are added.[32] As in other related non-covalent interactions, the bases can involve π-systems[33-35] or radicals,[36] as well as the more common lone pairs. Charge–assisted triel bonding interactions were found in search for the Cambridge Structural Database.[37] Triel bonding was also described as a "hidden interaction" in some circunstances.[38]

Given the strength with which both carbenes and triels can engage in intermolecular interactions individually, it is natural to wonder how they might interact with one another, and if so what would be the precise nature of such a bond. Would such an interaction have unique properties, in addition to its potential strength? Is it possible to predict the effects of substituents on each molecule, based on simple notions of electron-withdrawing or releasing properties? As $TrR_3$ molecules typically engage in large scale geometric deformation, it would be interesting to determine the extent of this distortion when bonding to a carbene, and how these changes might affect the nature of the interaction. How does the C lone pair of a carbene differ in its non-covalent bonding from the lone pairs of more common electron donor atoms N and O? It would also be interesting to determine how the interaction might be affected if the carbene C and its lone pair is replaced by the larger Si atom. This work addresses these questions via quantum chemical calculations applied to a large set of systems that are systematically chosen.

## 2. SELECTION OF SYSTEMS AND THEORETICAL METHODS

The basic carbene unit studied is part of a N-heterocyclic ring, cyclic CNHCHCHNH (abbreviated NHC), in which the carbene C is bracketed by a pair of NH units and then a pair of CH groups, as illustrated in Scheme I. The carbene C was replaced by Si in order to examine the corresponding silylene. F atoms were used to replace H in both the flanking N and C positions so as to examine substituent effects. Both triel (Tr) atoms B and Al were examined in the context of $TrR_3$ molecules, with R= H, F, Cl, Br, $CH_3$ in order to study substituent effects on the electron acceptor unit.

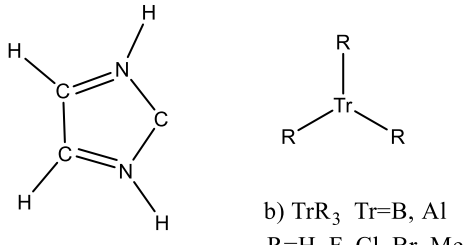


a) carbene NHC

b) $TrR_3$ Tr=B, Al
R=H, F, Cl, Br, Me

Scheme I

The structures of the monomers and complexes were fully optimized at the MP2/aug-cc-pVDZ level. Frequency calculations at the same level confirmed these structures to be true minima, and yielded zero-point vibrational energy (ZVE), as well as Gibbs free energy. To obtain more accurate results, these structures were then optimized at the MP2/aug-cc-pVTZ level. The interaction energy ($E_{int}$) was defined as the difference of energy between the complex and the corresponding monomers with their geometries in that of the complex. The binding energy ($E_b$) used the optimized monomer geometries as a reference point. Both $E_{int}$ and $E_b$ were corrected for basis set superposition error (BSSE) by the counterpoise method.[39] All calculations were carried out using the Gaussian 09 software.[40]

Molecular electrostatic potentials (MEPs) of the various monomers were evaluated on the 0.001 electrons/bohr$^3$ isodensity surface via the WFA-SAS program[41] at the B3LYP/6-31G(d) level. (These properties show remarkably little sensitivity to the specific theoretical level.[42]) Natural bond orbital (NBO) analysis was performed at the HF/aug-cc-pVTZ level via the NBO3.0 program[43] in Gaussian09 to estimate orbital interactions and charge transfer (CT). Atoms in molecules (AIM) treatment of the electron density topography at bond critical point (BCP) was carried out with the AIM2000 software.[44] The total interaction energy was decomposed into its various components at the MP2/aug-cc-pVTZ level with the LMOEDA (Localized Molecular Orbital-Energy Decomposition Analysis) method[45] in the GAMESS program.[46]

## 3. RESULTS

### 3.1. Monomer MEP analysis

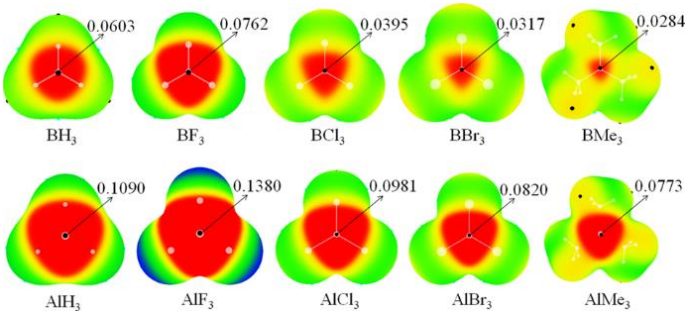


**FIGURE 1** MEP maps of $ZX_3$. Color ranges, in au, are: red, greater than 0.02; yellow, between 0.02 and 0; green, between 0 and -0.02; blue, smaller than -0.02.

The molecular electrostatic potentials (MEPs) of the various $TrR_3$ monomers (Tr=B, Al) are presented in FIGURE 1 wherein the most positive regions are designated by a red color. These potentials share the common feature of a red region of positive density directly above the Tr atom (and another below), which are designated π-holes[32] due to their location. As indicated by the labels in FIGURE 1, the intensity of this π-hole increases in the order of

substituent R = Me < Br < Cl < H < F for either triel atom. The rise with growing electron-withdrawing power of the halogen substituents is similar to that reported previously.[31] The surprisingly small values of $V_{s,max}$ in comparison to R=H may be due to backbonding from the halogen π-orbital into the p-orbital of Tr (from the C-H σ orbital in the case of R=Me).[30] Such hyperconjugation is supported by a NBO orbital interaction energy, equal for example to 46.22 and 11.45 kcal/mol in $BMe_3$ and $AlMe_3$, respectively. For a given R, $AlR_3$ has larger π-holes than $BR_3$ due to the lesser electronegativity and larger polarizability of Al relative to B. This difference in $V_{s,max}$ is on the order of 0.05 au.

The corresponding MEPs of the carbenes are illustrated in FIGURE 2 where the carbene C atom at the top of each diagram is surrounded by a negative (blue) potential. The area occupied by this negative region corresponds closely to the position of the C lone pair in the singlet carbene. The absolute value of $V_{s,min}$ is reduced by the placement of F atoms on the ring, due to its electron-withdrawing action, particularly when the F atoms are close to the relevant C. The lower electronegativity of Si as compared to C has an even stronger effect in reducing $V_{s,min}$, suggesting the silylene to be a poorer electron donor.

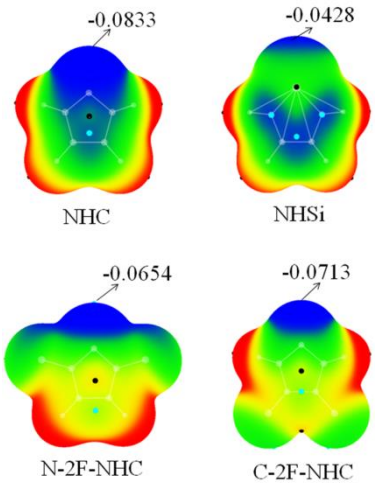


**FIGURE 2** MEP maps of NHC and its derivatives. Color ranges, in au, are: red, greater than 0.02; yellow, between 0.02 and 0; green, between 0 and -0.02; blue, smaller than -0.02.

### 3.2. Geometries and interaction energies

Given the nature of the electrostatic potentials, one would expect the carbene C lone pair to directly approach the triel atom from above, in what might be called a carbene triel bond. Optimization of two such pairs of molecules leads to the representative geometries displayed in FIGURE 3. The C/Si···Tr equilibrium distances for the full set are collected in the first column of Table 1. As a first marker of an attractive interaction, these distances are much

shorter (1.59-2.614 Å) than the sum of the van der Waals radii of the corresponding atoms (3.83 Å for C···B, 4.21 Å for C···Al, 4.23 Å for Si···B, 4.61 Å for Si ···Al).

**TABLE 1** Intermolecular distance (R, Å), ∑α (degs), and deformation energy (DE, kcal/mol)

| Complexes | R | ∑α | DE |
|---|---|---|---|
| NHC···$BH_3$(**15**) | 1.593 | 335.4 | 18.96 |
| NHC···$BF_3$(**16**) | 1.659 | 336.6 | 36.12 |
| NHC···$BCl_3$(**17**) | 1.602 | 336.0 | 33.04 |
| NHC···$BBr_3$(**18**) | 1.590 | 336.5 | 29.82 |
| NHC···$AlH_3$(**19**) | 2.027 | 348.3 | 7.62 |
| NHC···$AlF_3$(**20**) | 2.042 | 344.9 | 12.86 |
| NHC···$AlCl_3$(**21**) | 2.027 | 344.1 | 12.77 |
| NHC···$AlBr_3$(**22**) | 2.020 | 344.5 | 11.95 |
| N-2F-NHC···$BH_3$(**23**) | 1.594 | 337.7 | 16.78 |
| N-2F-NHC···$AlH_3$(**24**) | 2.131 | 351.1 | 5.51 |
| C-2F-NHC···$BH_3$(**25**) | 1.591 | 336.1 | 18.30 |
| C-2F-NHC···$AlH_3$(**26**) | 2.088 | 349.5 | 6.99 |
| N-2F-NHC···$BMe_3$(**27**) | 1.634 | 335.3 | 22.15 |
| N-2F-NHC···$AlMe_3$(**28**) | 2.152 | 350.5 | 5.74 |
| NHSi···$BH_3$(**29**) | 1.976 | 343.7 | 12.87 |
| NHSi···$AlH_3$(**30**) | 2.614 | 354.5 | 3.80 |

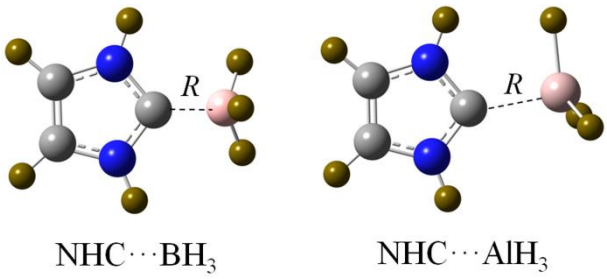


**FIGURE 3**. The optimized structures of NHC···$BH_3$ and NHC···$AlH_3$

As indicated in FIGURE 3 for the $TrH_3$ units, the $C_3$ axis of the $BR_3$ molecule is essentially collinear with the C lone pair, i.e. the CNC bisector, but $AlR_3$ tips up toward one of the two NH groups of the carbene. The latter reorientation permits an attractive interaction between the acidic carbene NH and one R atom of $AlR_3$ that will be slightly negative charged. This interaction would be termed a NH···X H-bond when R is a halogen X, and a dihydrogen bond for R=H, the latter of which is consistent with earlier work.[47] This latter interaction can be considered a small supplement to the carbene triel bond.

The energetics of the various complexes are collected in Table 2. The nature of the interaction leads to significant geometric deformation within the monomers, discussed at

some length below. The interaction energy between the two pre-deformed monomers, $E_{int}$, is thus significantly more exothermic than is the binding energy $E_b$ which references the monomers in their optimized structures, and corresponds to the formal ΔE for the combination reaction. $E_{int}$ varies from 20 kcal/mol for NHSi···$AlH_3$ all the way up to nearly 90 kcal/mol for NHC···$BBr_3$, with $E_b$ a bit less, covering the range from 16 to 58 kcal/mol. Because the reaction involves the transformation from a pair of molecules to a single complex, ΔS is negative for these reactions, so ΔG is considerably less exothermic than the binding energy itself, by an amount varying between 5 and 13 kcal/mol.

**TABLE 2** Interaction energy, $E_{int}$, binding energy, $E_b$, zero-point vibrational energy, ZVE, and Gibbs free energy at 298 K, ΔG, for complexation reaction (kcal/mol) and charge transfer (CT, e) between molecules

| Complexes | $E_{int}$ | $E_b$ | $E_{int}^{ZVE}$ | ΔG | CT |
|---|---|---|---|---|---|
| NHC···$BH_3$(**15**) | -74.16 | -55.20 | -70.67 | -43.39 | 0.532 |
| NHC···$BF_3$(**16**) | -73.62 | -37.50 | -71.77 | -32.71 | 0.489 |
| NHC···$BCl_3$(**17**) | -86.55 | -53.51 | -84.38 | -45.15 | 0.537 |
| NHC···$BBr_3$(**18**) | -88.25 | -58.43 | -86.03 | -51.87 | 0.502 |
| NHC···$AlH_3$(**19**) | -50.18 | -42.56 | -47.78 | -29.51 | 0.341 |
| NHC···$AlF_3$(**20**) | -68.33 | -55.47 | -66.40 | -44.69 | 0.220 |
| NHC···$AlCl_3$(**21**) | -70.44 | -57.67 | -68.58 | -48.72 | 0.270 |
| NHC···$AlBr_3$(**22**) | -69.82 | -57.87 | -68.01 | -49.58 | 0.262 |
| N-2F-NHC···$BH_3$(**23**) | -58.49 | -41.71 | -54.90 | -29.68 | 0.493 |
| N-2F-NHC···$AlH_3$(**24**) | -35.06 | -29.55 | -32.76 | -17.48 | 0.244 |
| C-2F-NHC···$BH_3$(**25**) | -70.83 | -52.53 | -67.49 | -40.76 | 0.520 |
| C-2F-NHC···$AlH_3$(**26**) | -46.57 | -39.58 | -44.25 | -26.43 | 0.256 |
| N-2F-NHC···$BMe_3$(**27**) | -44.65 | -22.50 | -41.70 | -10.30 | 0.500 |
| N-2F-NHC···$AlMe_3$(**28**) | -30.96 | -25.22 | -29.08 | -12.12 | 0.227 |
| NHSi···$BH_3$(**29**) | -39.90 | -27.03 | -37.71 | -15.35 | 0.844 |
| NHSi···$AlH_3$(**30**) | -20.26 | -16.46 | -18.68 | -5.45 | 0.383 |

There are a number of trends apparent in the data. In the first place, one can see from the bottom of Table 2 that the interaction of either $BH_3$ or $AlH_3$ with the silylene is far less exothermic than is the case with the carbene. With respect to the carbenes, $BR_3$ systematically engages in a stronger interaction energy than its $AlR_3$ analogues, opposite to the trend in $V_{s,max}$ in FIGURE 1. This opposite pattern is unique to these carbenes, as $AlX_3$ normally forms a stronger triel bond than $BX_3$.[31,33,48] On the other hand, the binding energies which reference the monomers in their optimized geometries do not echo this trend. Although $E_b$ is smaller for $AlH_3$ vs $BH_3$, this distinction disappears for the $TrX_3$ molecules, with X a halogen substituent.

As far as the R substituents go, the interactions of $AlR_3$ are not much affected by the nature of the halogen atoms. In the case of $BR_3$, however, the interactions are weakened as the halogen becomes more electron-withdrawing, a surprising trend in that the π-hole over the B atom becomes more intense (see FIGURE 1). This opposite trend, along with that noted above concerning B vs Al, is a strong indicator that the interaction is composed of far more than a simple electrostatic attractive force in these carbene triel bonds. And indeed prior work involving electron donors other than carbenes, e.g. $C_2H_4$ and $CH_3$, found that the interaction grows in the more expected order of X = Br < Cl < F.[33,48]

One of the features of triel bonds is a significant deformation of the $TrR_3$ monomer upon complexation, and these interactions with a carbene are no exception. This monomer is planar but becomes pyramidal upon formation of the complex. One can measure this nonplanarity via the sum of the three θ(X-Z-X) angles in $TrX_3$, Σα. This sum is of course 360° when planar, and its deviation from this amount corresponds to the degree of nonplanarity. The values of Σα in the various complexes are reported in the penultimate column of Table 1 where it differs quite a bit from 360°. It may first be noted that the $BR_3$ complexes are subject to greater deformation than their $AlR_3$ counterparts. This measure of deformation is generally proportional to the deformation energy (FIGURE 4), with a correlation coefficient of 0.98, if one ignores the three NHC···$BX_3$ complexes with disproportionately high deformation energy.

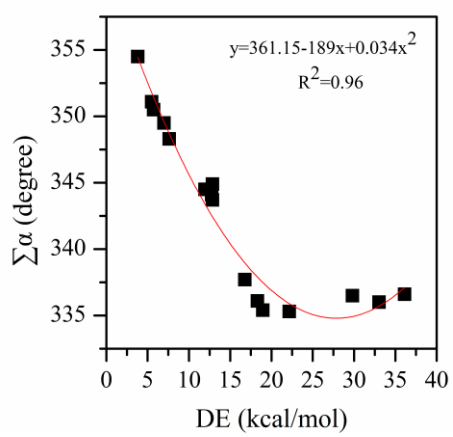


**FIGURE4** Relation between the Σα parameter and the deformation energy (DE)

With respect to substitutions on the carbene, one would expect that replacement of H by F ought to remove density from the carbene lone pair, and thus weaken the triel bond. This trend is in fact observed. When a pair of such H→F substitutions are made on the N atoms flanking the carbene C, the interaction energy drops by some 15 kcal/mol, whether B or Al. This decrement is smaller, only about 3 kcal/mol when the substitutions are made on the C atoms that are further away from the carbene C. Substitution by methyl groups on the triel

molecule also reduces the interaction energy, consistent with the idea that these electron-releasing groups will reduce the ability of the triel atom to accept electron density from the carbene.

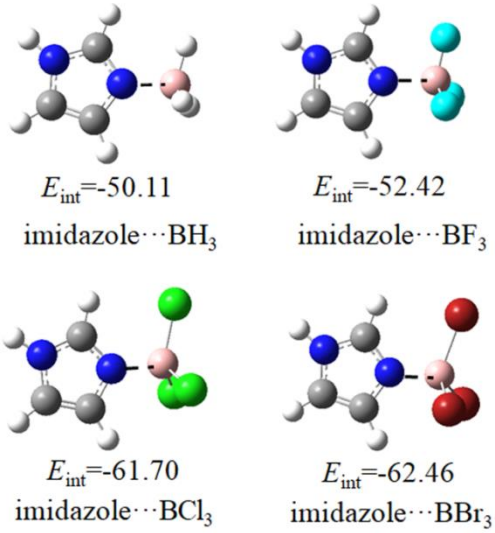


**FIGURE 5** The optimized structures of imidazole···$BX_3$. The interaction energies are in kcal/mol

NHC is essentially a tautomer of imidazole, wherein the H atom is moved from the C atom between the two N atoms to one of the N atoms, thereby changing from a system containing a N lone pair to a C lone pair. It would thus be of fundamental interest to examine how this tautomerization affects the properties of the triel bond. For this purpose the $BR_3$ molecules were chosen, with R=H, F, Cl, Br. Their complexes with the N lone pair of imidazole are displayed in FIGURE 5. The interaction energies of $BR_3$ with imidazole are all smaller in magnitude by 21-26 kcal/mol than their carbene counterparts in Table 2, representing a 30% reduction. This decrease is sensible for a number of reasons. In the first place, the greater electronegativity of N vs C would make the lone pair of the former less available for donation to $BR_3$. With respect to the MEP, $V_{s,min}$ at the N lone pair of imidazole is equal to -0.0723 au, less negative than that on the C lone pair in NHC (-0.0833 au). This reduced value would tend to reduce the electrostatic interaction within the dimer. Whether C or N lone pair, the interaction weakens in the order of R substituents on $BR_3$: F < Cl < Br. The only difference arises for R=H in that the interaction energy is weaker than R=F for the N lone pair, but stronger for the carbene.

### 3.3. Analysis of electronic structures

One common means to quantify the strength of a given bond is via an AIM analysis of the electron density topography. The molecular graphs of the various complexes are displayed in FIGURE 6, each of which verifies the presence of a bond path linking the triel atom with

the C/S of the carbene/silylene. The value of the electron density at the bond critical point is contained in Table 3, along with its Laplacian and the energy density, all measures of the bond strength. These quantities are large in the context of noncovalent bonds, generally exceeding for example the values normally observed for H-bonds.[49] As is typical,[50] $\rho_{BCP}$ displays an exponential relationship with the binding distance (FIGURE7). Based on the signs of the various quantities, these carbene triel bonds might be classified as partially covalent,[51] consistent with the previous conclusion.[52]

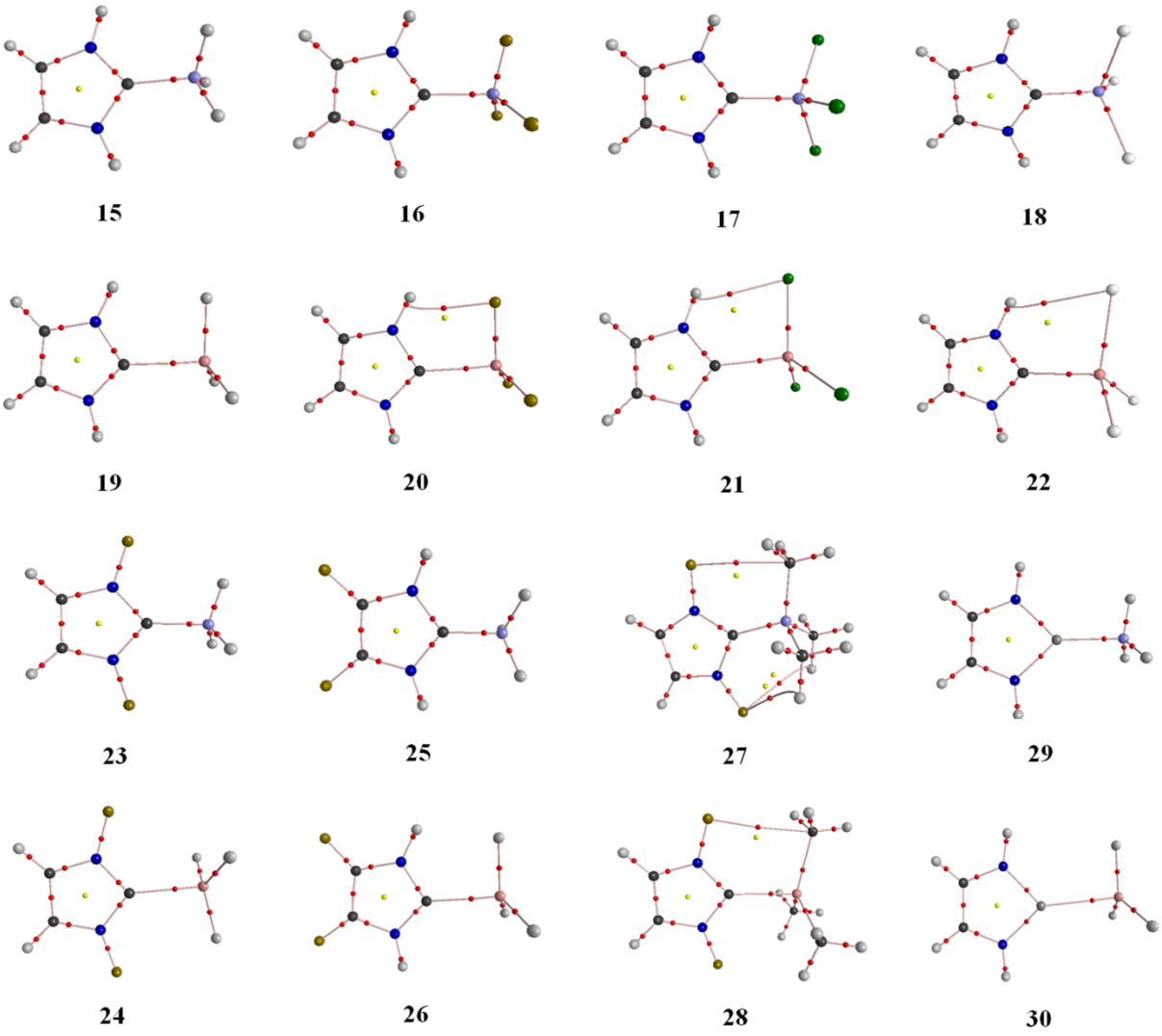


**FIGURE 6** The AIM molecular diagrams of the carbene triel-bonded complexes

**TABLE 3** Electron density (ρ**,** au), Laplacian ($\nabla^2\rho$, au), and energy density (*H*, au) at the intermolecular BCP

| Complexes | ρ | $\Delta^2\rho$ | H |
|---|---|---|---|
| NHC···$BH_3$(**15**) | 0.144 | 0.380 | -0.119 |
| NHC···$BF_3$(**16**) | 0.140 | 0.136 | -0.127 |
| NHC···$BCl_3$(**17**) | 0.164 | 0.656 | -0.159 |
| NHC···$BBr_3$(**18**) | 0.168 | 0.672 | -0.165 |
| NHC···$AlH_3$(**19**) | 0.058 | 0.284 | -0.006 |
| NHC···$AlF_3$(**20**) | 0.065 | 0.312 | -0.010 |
| NHC···$AlCl_3$(**21**) | 0.070 | 0.328 | -0.013 |
| NHC···$AlBr_3$(**22**) | 0.071 | 0.336 | -0.013 |
| N-2F-NHC···$BH_3$(**23**) | 0.135 | 0.452 | -0.104 |
| N-2F-NHC···$AlH_3$(**24**) | 0.049 | 0.248 | -0.003 |
| C-2F-NHC···$BH_3$(**25**) | 0.143 | 0.404 | -0.117 |
| C-2F-NHC···$AlH_3$(**26**) | 0.065 | 0.280 | -0.006 |
| N-2F-NHC···$BMe_3$(**27**) | 0.123 | 0.428 | -0.089 |
| N-2F-NHC···$AlMe_3$(**28**) | 0.046 | 0.236 | -0.002 |
| NHSi···$BH_3$(**29**) | 0.103 | -0.002 | -0.089 |
| NHSi···AlH3(30) | 0.033 | 0.088 | -0.006 |

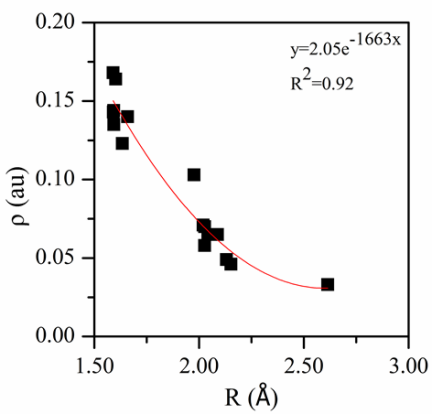


**FIGURE 7** Electron density (ρ) at the C/Si···Tr BCP versus the intermolecular distance (R)

In addition to the triel bond paths in FIGURE 6, several of the complexes display a secondary bond path between a halogen atom of $AlX_3$ and a NH proton on the carbene. It is this NH··X H-bond that is largely responsible for the aforementioned nonlinearity between the NCN bisector of the carbene and the $C_3$ axis of $AlX_3$. Another interesting secondary attraction is noted in **27** and **28** wherein a bond path connects the F atom on the substituted carbene and the methyl C on the $TrMe_3$, with $\rho_{BCP}$ = 0.008 and 0.005 au, respectively, which could perhaps be categorized as a weak tetrel bond.[53-55]

Another element involved in the interaction is the total amount of charge that is transferred from the carbene to the $TrR_3$ Lewis acid (CT). As may be noted by the last

column of Table 2, this quantity is rather large, up to as much as 0.5 e in a number of cases, and even exceeding 0.8 e for NHSi···$BH_3$. The charge transfer is uniformly much larger for Tr=B than for Al, by roughly a factor of 2. There is no clear correlation between the magnitude of CT and the interaction or binding energies as different substituents R are placed on the $TrR_3$.

To confirm the contribution of orbital interactions, we performed a calculation of energy decomposition analysis (EDA) in conjunction with an analysis of natural orbital for chemical valence (NOCV) with ADF2008.01 program.[56] The orbital interactions can be classified as two types of NHC→B/Al donation and B/Al→NHC back-donation, and we only analyze two strongest donation and back-donation interactions. The plots of the deformation densities (Δρ) associated with the two orbital interactions are shown in FIGURE 8 with two examples of NHC···$BH_3$ and NHC···$AlH_3$ in which electron density is shifted from red to blue regions. The NHC→B/Al donation interaction is much stronger than the B/Al→NHC back-donation interaction, indicating that the carbene triel bond is like other type of triel bond although it is very strong. The donation and back-donation contribution in NHC···$BH_3$ is larger than that in NHC···$AlH_3$, consistent with the interaction energy. This shows that the orbital interaction is important in the carbene triel bond.

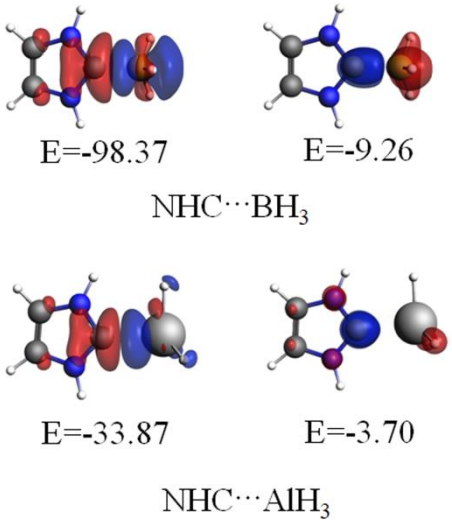


**FIGURE 8** Plots of deformation densities of the pair-wise orbital interactions (Δρ) in NHC···$BH_3$ and NHC···$AlH_3$ at the PBED3/TZ2P//MP2/aug-cc-pVTZ level[57]. The associated orbital interaction energies are given in kcal/mol. The color code of the charge flow is red→blue and the isovalue for Δρ(r) is 0.002 au.

**TABLE 4** Electrostatic (ES), exchange (EX), repulsion (REP), polarization (POL), and dispersion (DISP) energies. All are in kcal/mol

| Complexes | ES | EX | REP | POL | DISP |
|---|---|---|---|---|---|
| **15** | -119.80 | -183.04 | 348.55 | -106.07 | -13.73 |
| **16** | -134.83 | -149.44 | 313.97 | -101.51 | -1.74 |
| **17** | -165.60 | -230.00 | 464.74 | -143.81 | -11.74 |
| **18** | -176.02 | -254.42 | 512.21 | -155.99 | -14.24 |
| **19** | -87.00 | -82.82 | 162.87 | -36.98 | -6.80 |
| **20** | -101.89 | -61.82 | 137.49 | -40.73 | -1.53 |
| **21** | -111.17 | -94.62 | 193.35 | -50.84 | -7.38 |
| **22** | -115.87 | -108.60 | 218.25 | -55.03 | -9.37 |
| **23** | -97.86 | -165.23 | 317.61 | -97.58 | -14.74 |
| **24** | -59.40 | -64.02 | 125.06 | -30.27 | -6.59 |
| **25** | -115.71 | -179.13 | 342.46 | -103.75 | -14.62 |
| **26** | -81.35 | -80.15 | 157.74 | -35.36 | -7.64 |
| **27** | -103.21 | -180.65 | 347.09 | -88.27 | -19.97 |
| **28** | -57.29 | -67.30 | 129.15 | -26.90 | -9.08 |
| **29** | -65.52 | -152.28 | 284.16 | -91.90 | -14.62 |
| **30** | -36.41 | -54.97 | 102.57 | -26.55 | -4.96 |

The decomposition of the total interaction energy into its various physically meaningful components can offer certain insights into the nature of the binding. These components are collected in Table 4 where a number of trends are readily apparent. In the first place, all of the terms are larger for the B systems than for Al. In terms of the individual components, ES stands as the most attractive for Tr=Al but EX surpasses ES for Tr=B. POL is third in this hierarchy, nearly as large as ES for Tr=B but considerably smaller for the Al analogues. Dispersion is the smallest of the four, and by a good deal. The situation changes for the silylenes in the last two rows of Table 4, particularly for NHSi···$BH_3$ where ES is surpassed by both EX and POL. The relative contributions of these terms is similar to that observed in carbene tetrel bonds NHC···$TH_3F$ (T = Si, Ge, and Sn).[15]

## 4. DISCUSSION AND CONCLUSIONS

The combination of a $TrR_3$ molecule with a N-heterocyclic carbene leads to a strong triel bond, with interaction energies that range all the way up to nearly 90 kcal/mol. The interaction leads to substantial deformation of the $TrR_3$ unit so the energy of the binding reaction is a bit lower, but still as high as 60 kcal/mol. The energy required to distort the $TrR_3$ molecule into the geometry it adopts within the context of the dimer is larger for Tr=B than for Al, particularly with halogen substituents R. Lots of charge is transferred from the base to the acid, as much as 0.5 e. Unlike many other non-covalent interactions, there is no clear correlation between the electron-withdrawing power of substituents on the

electron-accepting Lewis acid and the strength of the binding, and in some cases the expected trend is reversed. On the other hand, the expected pattern is observed for carbene substitution, wherein electron-withdrawing substituents on the Lewis base weaken the interaction. Replacement of the C lone pair of the carbene by a silylene weakens the interaction, despite the lesser electronegativity of Si as compared to C, which ought to amplify the accessibility of its lone pair. A weakening of the interaction also occurs when the C lone pair of the carbene is replaced by the N lone pair in the imidazole tautomer. When these anomalous trends are placed in the context of the large densities at the bond critical points, short intermolecular distances, and large interaction energies, some of these carbene triel bonds may be considered as borderline covalent in nature.

There are results in the literature that help place some of our trends in a broader perspective, and which underscore the strength of the intermolecular interactions in which carbenes engage. The interaction energy involved in thetriel bond between $TrX_3$ and a π electron donor such as $C_2H_4$, $C_2H_2$, or $C_6H_6$ is much smaller than for the carbenes here, less than -22 kcal/mol.[33,34] The interaction energy of the triel bond between $TrX_3$ and the $CH_3$radical is less than -13 kcal/mol.[48] Clearly, both types of electron donors engage in a weaker triel bond than does NHC. The interaction energy is less than -50.4 kcal/mol when $BX_3$ binds with $NH_3$,[58] which is smaller than that in NHC⋯$BX_3$, further supporting the notion that a carbene C lone pair is a stronger nucleophile than is the N lone pair.

The binding of $TrH_3$ and $TrX_3$ (Tr = B and Al, X=halogen), with the weak base HCN[31] leads to interaction energies that are much smaller than those here, less than 30 kcal/mol, as well as including lesser amounts of charge transfer. Interestingly, whereas the B center engages in a stronger triel bond than the Al analogue for $TrH_3$, this pattern reverses for $TrX_3$, a pattern which is observed also for the $Me_3N$ base.[22] This behavior contrasts with our finding that both $BH_3$ and $BX_3$ form a stronger carbene triel bond than does its Al congener. We note also that halogen substitution enhances the triel carbene bond, whether B or Al, whereas the opposite is observed for the interaction between B and HCN[31]. The strong basicity of the C lone pair in the NHC is underscored by its stronger triel bond than even the very strongly basic $Me_3N$. Its binding energy of 49.3 kcal/mol with $AlCl_3$[22] is eclipsed by our value of 70.4 kcal/mol for NHC⋯$AlCl_3$. The propensity of carbenes to engage in strong noncovalent interactions is apparent also in its tetrel bonds with $TH_3F$ (T = C, Si, Ge, Sn),[15] where it surpasses the binding of strong bases such as $NH_3$.

For most types of triel-bonded complexes, both electrostatic and polarization components are linearly related to the total interaction energy.[48,58] The expected linear relationship is noted here by the black points in FIGURE9 for the electrostatic component, but polarization energy (red) fails to obey this pattern. It was demonstrated earlier that derivatives of $(H_3P{=}N)_2Si$ are powerful neutral superbases.[59] The charge transfer in pnicogen bonding with

silylene (>0.3e)[60] is much larger than that in pnicogen bonding with carbene (<0.1e),[61] leading to the supposition that charge transfer is enhanced when the C atom of the carbene is changed to Si.

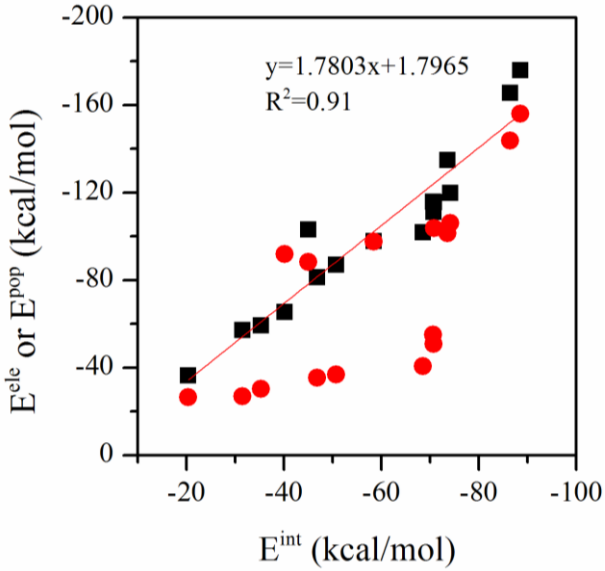


**FIGURE 9** Relationship of the interaction energy with the electrostatic (black) and polarization (red) components. Function refers to linear correlation of the electrostatic data

Curran et.al.[62] presented a detailed review on the synthesis and reactions of N-heterocyclic carbene boranes (NHC-boranes), where they enumerated their examples as reactants in acid/base reactions, reactions of NHC-boranes with electrophiles, nucleophilic substitutions of boryl halides and sulfonates, electrophilic substitutions of boryl anions, reactions with metal complexes, and elimination reactions as well as reagents and catalysts in radical reactions, ionic reactions, and organometallic reactions, and they concluded that NHC-boranes are promising as reagents and catalysts in organic synthesis and as co-initiators in radical polymerization. More applications of NHC-boranes have been reported.[63,64] Our theoretical results for NHC-boranes and its silicon or aluminium derivatives are helpful for understanding their functions in the above applications and developing their new roles.

## ACKNOWLEDGEMENTS

This work was supported by the National Natural Science Foundation of China (21573188) and the Open Subject of Faculty of Chemistry of QingDao University of Science and Technology (QUSTHX201807).

[1] W. A. Herrmann, C. Köcher, *Angew. Chem. Int. Ed*. **1997**, *36*, 2162.
[2] W. A. Herrmann, *Angew. Chem. Int. Ed*. **2002,** *41*, 1290.
[3] N. Marion, S. P. Nolan, *Chem. Soc. Rev*. **2008**, *37*, 1776.

[4] S. Díez-González, N. Marion, S. P. Nolan, *Chem. Rev*. **2009**, *109*, 3612.
[5] D. Enders, O. Niemeier, A. Henseler, *Chem. Rev.* **2007**, *107*, 5606.
[6] N. Marion, S. Díez-González, S. P. Nolan, *Angew. Chem. Int. Ed.* **2007**, *46*, 2988.
[7] M. N. Hopkinson, C. Richter, M. Schedler, F. Glorius, *Nature* **2014**, *510*, 485.
[8] I. Alkorta, J. Elguero, *J. Phys. Chem.* **1996**, *100*, 19367.
[9] Q.Z. Li, Y.L. Wang, Z.B. Liu, W.Z. Li, J.B. Cheng, B.A. Gong, J.Z. Sun, *Chem. Phys. Lett.* **2009**, *469*, 48.
[10] M.D. Esrafili, N. Mohammadirad, *J. Mol. Model*. **2013**, *19*, 2559.
[11] Q.Z. Li, H.Z. Wang, Z.B. Liu, W.Z. Li, J.B. Cheng, B.A. Gong, J.Z. Sun, *J. Phys. Chem. A* **2009**, *113*, 14156.
[12] Z.F. Li, S. Yang, H.X. Li, *J. Mol. Struct. THEOCHEM* **2010**, *952*, 56.
[13] Q. Zhao, D.C. Feng, Y.M. Sun, J.C. Hao, Z.T. Cai, *Int. J. Quant. Chem*. **2011**, *111*, 3881.
[14] B. Pinter, N. Nagels, W.A. Herrebout, F. De Proft, *Chem. Eur. J.* **2013**, *19*, 519.
[15] M.X. Liu, Q.Z. Li, W.Z. Li, J.B. Cheng, *Struct. Chem*. **2017**, *28*, 823.
[16] J. E. Del Bene, I. Alkorta, J. Elguero, *J. Phys. Chem. A* **2017**, *121*, 4039.
[17] J. E. Del Bene, I. Alkorta, J. Elguero, *J. Phys. Chem. A* **2017**, *121*, 8136.
[18] I. Alkorta, M. M. Montero-Campillo, J. Elguero, *Eur. Chem. J.* **2017**, *23*, 10604.
[19] M.X. Liu, Q.Z. Li, J.B. Cheng, W.Z. Li, H.B. Li, *J. Chem. Phys.* **2016**, *145*, 224310.
[20] Z. Guo, Na R. Song, J. H. Moon, M. Kim, E. J. Jun, J. Choi, J. Y. Lee, C. W. Bielawski, J. L. Sessler, J. Yoon, *J. Am. Chem. Soc.* **2012**, *134*, 17846.
[21] I. R. Beattie, P. J. Jones, *Angew. Chem. Int. Ed.* **1996**, *35*, 1527.
[22] V. Jonas, G. Frenking, M. T. Reetz, *J. Am. Chem. Soc*. **1994**, *116*, 8741.
[23] W. A. Burns, K. R. Leopold, *J. Am. Chem. Soc.* **1993**, *115*, 11622.
[24] H.J. Jiao, P. v. R. Schleyer, *J. Am. Chem. Soc.* **1994**, *116*, 7429.
[25] S. W. Reeve, W. A. Burns, F. J. Lovas, R. D. Suenram, K. R. Leopold, *J. Phys. Chem.* **1993**, *97*, 10630.
[26] D. L. Fiacco, Y. Mo, S. W. Hunt, M. E. Ott, A. Roberts, K. R. Leopold, *J. Phys. Chem. A* **2001**, *105*, 484.
[27] G. Venter, J.Dillen, *J. Phys. Chem. A* **2004**, *108*, 8378.
[28] J. A. Phillips, D. J. Giesen, N. P. Wells, J. A. Halfen, C. C. Knutson, J. P. Wrass, *J. Phys. Chem. A* **2005**, *109*, 8199.
[29] H. Hirao, K. Omoto, H. Fujimoto, *J. Phys. Chem. A* **1999**, *103*, 5807.
[30] P. C. Hiberty, G. Ohanessian, *J. Am. Chem. Soc*. **1982**, *104*, 66.
[31] S. J. Grabowski, *ChemPhysChem* **2015**, *16*, 1470.
[32] S. J. Grabowski, *ChemPhysChem* **2014**, *15*, 2985.
[33] S.J. Grabowski, *Molecules* **2015**, *20*, 11297.
[34] S. J. Grabowski, *Struct. Chem.* **2017**, *28*, 1163.
[35] A. Bauzá, A. Frontera, *Theor. Chem. Acc*. **2017**, *136*, 37.
[36] M. D. Esrafili, P. Mousavian, *Chem. Phys. Lett.* **2017**, *678*, 275.
[37] A. Bauzá, X. García-Llinás, A. Frontera, *Chem. Phys. Lett*. **2016**, *666*, 73.
[38] E. C. Escudero-Adán, A. Bauzá, C. Lecomte, A. Fronterab, P. Ballester, *Phys. Chem.*

*Chem. Phys.* **2018**, *20*, 24192.
[39] S. F. Boys, F. Bernardi, *Mol. Phys.* **1970**, *19*, 553.
[40] M. J. Frisch, G. W. Trucks, H. B. Schlegel, G. E. Scuseria, M. A. Robb, J. R. Cheeseman, G. Scalmani, V. Barone, B. Mennucci, G. A. Petersson, H. Nakatsuji, M. Caricato, X. Li, H. P. Hratchian, A. F. Izmaylov, J. Bloino, G. Zheng, J. L. Sonnenberg, M. Hada, M. Ehara, K. Toyota, R. Fukuda, J. Hasegawa, M. Ishida, T. Nakajima, Y. Honda, O. Kitao, H. Nakai, T. Vreven, J. J. A. Montgomery, J. E. Peralta, F. Ogliaro, M. Bearpark, J. J. Heyd, E. Brothers, K. N. Kudin, V. N. Staroverov, R. Kobayashi, J. Normand, K. Raghavachari, A. Rendell, J. C. Burant, S. S. Iyengar, J. Tomasi, M. Cossi, N. Rega, J. M. Millam, M. Klene, J. E. Knox, J. B. Cross, V. Bakken, C. Adamo, J. Jaramillo, R. Gomperts, R. E. Stratmann, O. A. Yazyev, J. Austin, R. Cammi, C. Pomelli, J. W. Ochterski, R. L. Martin, K. Morokuma, V. G. Zakrzewski, G. A. Voth, P. Salvador, J. J. Dannenberg, S. A. Dapprich, D. Daniels, O. Farkas, J. B. Foresman, J. V. Ortiz, J. Cioslowski , D. J. Fox, Gaussian 09, Revision A.02, Gaussian, Inc. Wallingford, CT 2009.
[41] F.A. Bulat, A.Toro-Labbé, T. Brinck, J.S. Murray, P. Politzer, *J. Mol. Model.* **2010**, *16*, 1679.
[42] J. S. Murray, P. Politzer, *Wiley Interdisciplinary Rev*. **2011**, *1*, 153.
[43] A. E. Reed, L. A. Curtiss, F. F. Weinhold, *Chem. Rev*. **1988**, *88*, 899.
[44] F. Biegler-Konig, AIM2000; University of Applied Sciences. Bielefeld, Germany, 2000.
[45] P. F. Su, H. Li, *J. Chem. Phys.* **2009**, *131*, 014102.
[46] M.W. Schmidt, K.K. Baldridge, J.A. Boatz, S.T. Elbert, M.S. Gordon, J.H. Jensen, S. Koseki, N. Matsunaga, K.A. Nguyen, S. Su, T.L. Windus, M. Dupuis, J.A. Montgomery. *J. Comput. Chem.* **1993**, *14*, 1347.
[47] S. Marincean, J. E. Jackson, *J. Phys. Chem. A* **2004**, *108*, 5521.
[48] M. D. Esrafili, F. Mohammadian, *Struct. Chem*. **2016**, *27*, 1157.
[49] I. Alkorta, J. Elguero, *J. Phys. Chem. A* **1999**, *103*, 272.
[50] U. Koch, P. L. A. Popelier, *J. Phys. Chem. A* **1995**, *99*, 9747.
[51] W. D. Arnold, E. Oldfield, *J. Am. Chem. Soc*. **2000**, *122*, 12835.
[52] S. Sarmah, A. K. Guha, A. K. Phukan, *Eur. J. Inorg. Chem.* **2013**, 3233.
[53] M.X. Liu, Q.Z. Li, S. Scheiner, *Phys. Chem. Chem. Phys.* **2017**, *19*, 5550.
[54] A. Bauzá, A. Frontera, *Crystals* **2016**, *6*, 26.
[55] P. Pal, S. Konar, P. Lama, K. Das, A. Bauza, A. Frontera, S. Mukhopadhyay, *J. Phys. Chem. B* **2016**, *120*, 6803.
[56] ADF2008.01, SCM, Theoretical Chemistry, Vrije Universiteit, Amsterdam, The Netherlands, Available from: http://www.scm.com
[57] S. Grimme, J. Antony, S. Ehrlich, H. Krieg, *J. Chem. Phys*. **2010**, *132*, 154104
[58] S.J. Grabowski, *J. Comput. Chem.* **2018**, *39*, 472.
[59] A. K. Biswas, R. Lo, B. Ganguly, *J. Phys. Chem. A* **2013**, *117*, 3109.
[60] H.Y. Zhuo, Q.Z. Li, *Phys. Chem. Chem. Phys*. **2015**, *17*, 9153.
[61] J. E. Del Bene, I. Alkorta, J. Elguero, *ChemPhysChem* **2017**, *18*, 1597.

[62] D. P. Curran, A. Solovyev, M. M. Brahmi, L. Fensterbank, M. Malacria, E. Lacôte, *Angew. Chem. Int. Ed.* **2011**, *50*, 10294.
[63] T. Liu, L. Chen, Z. Sun, *J. Org. Chem*. **2015**, *80*, 11441.
[64] C.T. Shen, Y.H. Liu, S.M. Peng, C.W. Chiu, *Angew. Chem. Int. Ed*. **2013**, *52*, 13293.